



Molecular Crystals and Liquid Crystals

Publication details, including instructions for authors and subscription information:

<http://www.tandfonline.com/loi/gmcl20>

DEVICE FABRICATIONS OF ORGANIC THIN-FILM TRANSISTORS

Seong Hyun Kim^a, Jung Hun Lee^a, Yong Suk Yang^a
& Taehyoung Zyung^a

^a Basic Research Lab., ETRI, 161 Gajeong-Dong,
Yusong-Gu, Daejeon 305-350, Korea

Version of record first published: 15 Jul 2010

To cite this article: Seong Hyun Kim, Jung Hun Lee, Yong Suk Yang & Taehyoung Zyung (2003): DEVICE FABRICATIONS OF ORGANIC THIN-FILM TRANSISTORS, *Molecular Crystals and Liquid Crystals*, 405:1, 137-152

To link to this article: <http://dx.doi.org/10.1080/15421400390263587>

PLEASE SCROLL DOWN FOR ARTICLE

Full terms and conditions of use: <http://www.tandfonline.com/page/terms-and-conditions>

This article may be used for research, teaching, and private study purposes. Any substantial or systematic reproduction, redistribution, reselling, loan, sub-licensing, systematic supply, or distribution in any form to anyone is expressly forbidden.

The publisher does not give any warranty express or implied or make any representation that the contents will be complete or accurate or up to date. The accuracy of any instructions, formulae, and drug doses should be independently verified with primary sources. The publisher shall not be liable for any loss, actions, claims, proceedings, demand, or costs or damages

whatsoever or howsoever caused arising directly or indirectly in connection with or arising out of the use of this material.

DEVICE FABRICATIONS OF ORGANIC THIN-FILM TRANSISTORS

Seong Hyun Kim*, Jung Hun Lee, Yong Suk Yang,
and Taehyoung Zyung
Basic Research Lab., ETRI, 161 Gajeong-Dong, Yusong-Gu,
Daejeon 305-350, Korea

Organic TFTs with p-type pentacene and n-type F₁₆CuPc were fabricated on both Si and plastic substrates. Maximum p-type mobility of 0.8 cm²/Vs and 0.12 cm²/Vs were achieved for Si and plastic substrates, respectively. JSS-362 was used as a gate dielectrics for plastic substrate. To decrease the contact resistance between metal electrodes and organic semiconductors, self-assembled monolayers were formed. Charge carrier mobilities of the device with both pentacene and F₁₆CuPc were increased after SAMs treatments on metal contacts.

I. INTRODUCTION

Organic thin-film transistors (OTFTs) have been extensively studied for many applications such as display operation, identification tags, and sensors. The reasons why we investigate the organic transistors are their low cost and simpler packaging, relative to conventional inorganic electronics, and their compatibility with flexible substrates. P-type organic thin-film field-effect transistors (FETs) reached mobilities exceeding 1 cm²/Vs and on/off ratios of 10⁶ close to amorphous silicon FETs [1].

Scientists are now developing the displays composed of the organic light emitters and the OTFTs on flexible and sheer plastic sheets that can make the process cheap using a method such as silk-screening or ink-jet printing [2,3]. The applications of OTFTs include the switching devices in the pixels for active-matrix liquid crystal displays (AMLCDs) [4], and the

This work has supported financially by Korean Ministry of Science and Technology through the NRL program.

*Corresponding author. E-mail: kimsh@etri.re.kr

active-matrix backplanes for electronic paper (e-paper) display [5] containing the pixels made up of either micro-capsuled electrophoretic ink containing microcapsules [6] or “twisting balls” [7]. Key elements in the e-paper would be OTFTs which has the same properties as conventional silicon transistors except flexibility. Other applications of OTFTs include the low-end smart cards and the electronic identification tags.

In most digital circuitry, minimal power dissipation and stability of performance against transistor parameter variations are crucial. In silicon-based microelectronics, these are achieved through the use of complementary logic-which incorporate both p-and n-type transistors-and it is therefore reasonable to support that adoption of such an approach with organic semiconductors will similarly result in reduced power dissipation, improved noise margins and greater operational stabilities [8]. However, n-type FETs show much lower mobilities than p-type semiconductor, pentacene by an order of magnitude [9]. Despite recent improvements of n-channel materials the low mobility and stability still limit performance, especially speed, of complementary circuits. Therefore, searching for new n-type organic semiconductors with air-stability and high electron mobility (over $1\text{ cm}^2/\text{Vs}$) is essential. It is known that in order for a material to transport electrons, it needs to have an accessible LUMO level for electron injection and sufficient π -overlaps to achieve reasonable charge carrier mobilities [10]. Few years ago, hexadecafluorocopperphthalocyanine (F_{16}CuPc) was found to function as air-stable n-channel semiconductors with a maximum electron field-effect mobility of $0.03\text{ cm}^2/\text{Vs}$ [10].

It is well known that the formation of the metal/organic interface is one of the most important factors in determining the devices performance, since the charge injection into the semiconductor layer via the interface dependence on the quality of the contact formation [11]. Based on the mechanism of OTFT, the drain current, I_D , will show linear behavior at small bias, V_{DS} , along with the conductivity of the film, σ [12] when the metal-organic interface has ohmic contact. However, the non-ohmic contact property [11] makes the I_D non-linear behavior at low V_{DS} [13]. According to the previous report [11], regardless of deposition order, there is no chemical bonding between organic semiconductor, pentacene, and Au at the interface, but just a physical adsorption of Au atoms. They also reported that, when pentacene is deposited onto Au, there is an immediate shift of the vacuum level 0.91 eV closer to the fermi level that is attributed to an interface dipole of $\sim -1\text{ eV}$. This can make current injection at the contacts difficult.

To improve the contact properties between the organic semiconductors and the metal electrodes, modified drain- and source-contacts using charge transfer (CT) compounds through a self-assembly approach was

proposed [13]. Contact modification led to larger drain currents and better current saturation comparing to non-modified contacts.

In this work, three kinds of OTFTs were fabricated using n-type organic semiconductor, and the contacts have been modified with three different molecules using self-assembly technique and there effects on the transistors performances were reported.

II. EXPERIMENTAL

A highly conductive Si wafer (resistivity 5–10 Ωcm) is used both as a substrate and as a gate electrode. The gate dielectric layer for all the devices is thermally grown 300 nm-thick SiO_2 layer (capacitance per unit area $C_o = 10 \text{ nF/cm}^2$). As a plastic substrates, polyethylene naphthalate (PEN) films were used. Gate dielectrics for the devices on plastic substrates, several organic and inorganic dielectric layers such as thermal curable acrylate (JSS-362, Japan Synthetic Rubber, JSR), poly vinyl alcohol (PVA), Al_2O_3 , and AlO_xN_y were fabricated by using spin-coating technique for organics and sputtering for inorganic layers.

Ti(10 nm)/Au(80 nm) gate-, source- and drain-electrodes are photolithographically defined such that the channel width W is 50 μm and the channel length L is 10 μm . Figure 1(a) and (b) represent the schematic

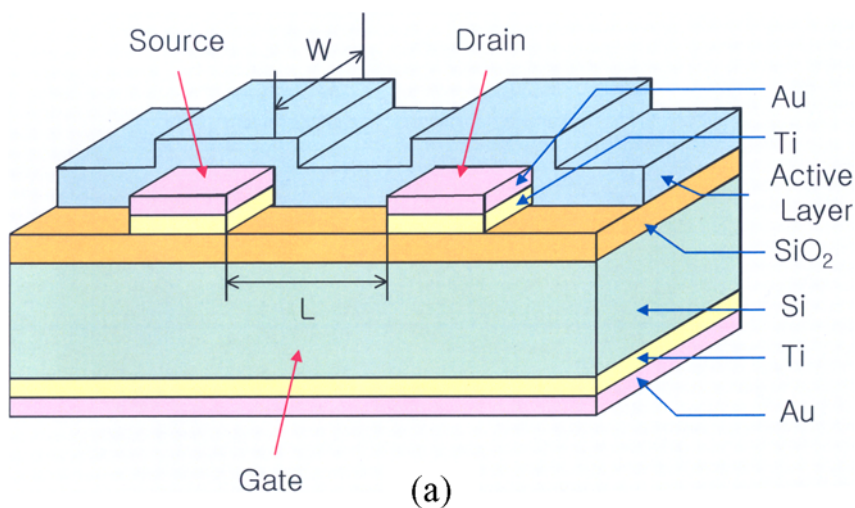


FIGURE 1 Schematic diagrams of organic TFTs on (a) Si substrate and (b) plastic substrate. Channel length and width are 10 μm and 50 μm , respectively. (See COLOR PLATE II)

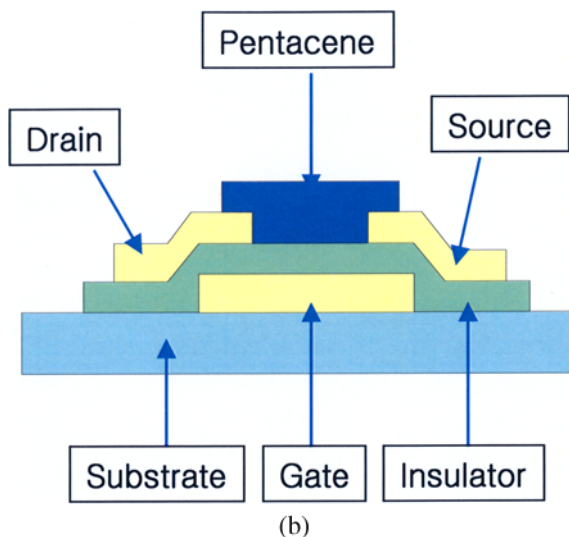


FIGURE 1 (Continued). (See COLOR PLATE III)

diagrams of the structures of organic field-effect transistor fabricated on Si and plastic substrates, respectively in this experiments.

For the treatments of the source- and drain-electrodes surfaces, three kinds of thiol compounds, 2-mercapto-5-nitrobenzimidazole (MNB), 2-mercaptobenzimidazole (MB), and 2-mercapto-5-methylbenzimidazole (MMB) were formed as a monolayer on the Au electrodes using self-assembly technique. Prior to the layering process, the electrode surfaces were cleaned by oxygen plasma ashing for 5 min. 0.2 molar solutions of the thiol compounds in ethanol were made and the pre-cleaned source- and drain-electrodes were immersed for 24 hours followed by rinsing by ultrasonication in pure ethanol and drying under an argon stream. The self-assembled monolayers (SAMs) can be selectively formed on the drain-source region, so that no additional patterning is required.

Active layers with pre-sublimed (purified) pentacene and hexadecafluorocopperphthalocyanine ($F_{16}CuPc$) are fabricated under the vacuum of less than 2×10^{-6} torr directly on the TFT substrate at the substrate temperatures of $60^\circ C$ for pentacene and $180^\circ C$ for $F_{16}CuPc$. Pentacene and $F_{16}CuPc$ are p- and n-type organic semiconductors, respectively. The thickness of both active layers is 100 nm using a deposition rate of 1 \AA/s . Transistor characteristics of the devices have been measured with a precision semiconductor parameter analyzer (4156c, Agilent) at room temperature in air.

III. RESULTS AND DISCUSSION

3.1. Device Fabrication – the Crystallization of Organic Layer

The pentacene thin films were deposited by using conventional thermal evaporator at the pressure below 10^{-6} Torr. The Si/SiO₂ substrates were treated with hexamethyldisilazane (HMDS) as the self-organizing materials, which had been used to improve the quality of the organic/dielectrics interface [14]. The substrate temperature was elevated and maintained at 60°C during the deposition. Figure 2 shows the surface morphology of the pentacene film observed by an atomic force microscope (AFM). The image was observed over the area of $10\text{ }\mu\text{m} \times 10\text{ }\mu\text{m}$ in a noncontact mode, and the scan frequency was 0.5 Hz. The pentacene film revealed dendritic grains.

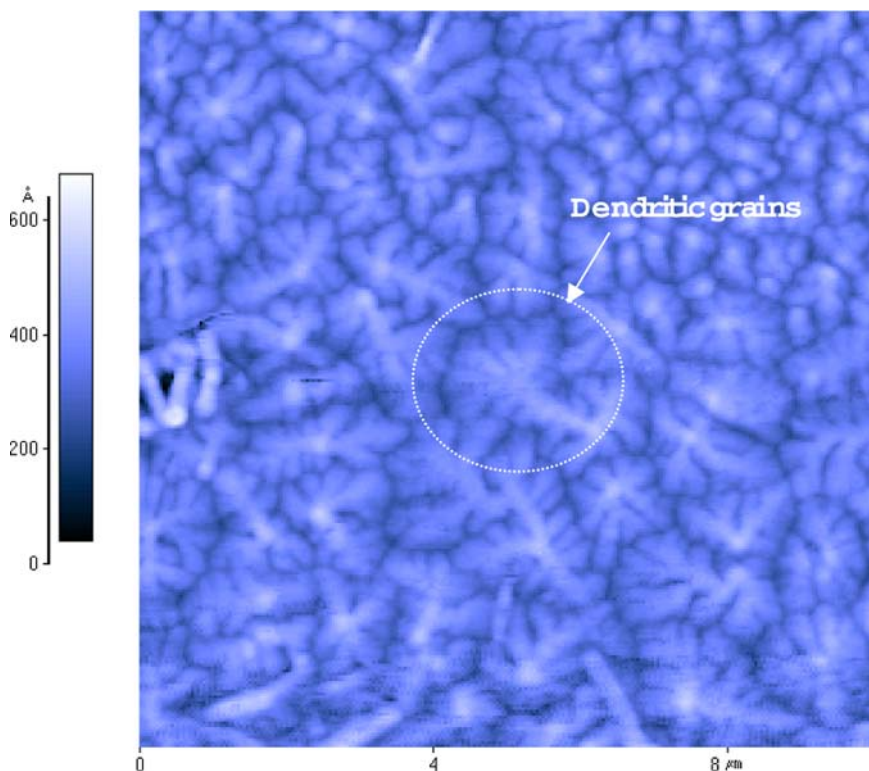


FIGURE 2 AFM image of the pentacene film with a thickness of 50 nm. The average grain size and rms roughness were approximately 2 nm and 51 Å. The image was observed over the area of $10\text{ }\mu\text{m} \times 10\text{ }\mu\text{m}$ in a noncontact mode, and the scan frequency was 0.5 Hz. (See COLOR PLATE IV)

The average grain size, root-mean-square surface roughness, and peak-to-valley roughness were 2 μm , 51 \AA , and 238 \AA , respectively. The film roughness did not increase significantly for the films thicker than 50 nm.

Figure 3 shows the X-ray diffraction (XRD) patterns of pentacene films deposited on Si/SiO₂ substrates. The samples were heat treated after deposition for further crystallization. The crystal structure of the pentacene is triclinic with $a = 7.90 \text{ \AA}$, $b = 6.06 \text{ \AA}$, $c = 16.01 \text{ \AA}$, $\alpha = 101.9^\circ$, $\beta = 112.6^\circ$, and $\gamma = 85.5^\circ$ [15]. Comparing the XRD pattern observed in this experiments with previous report [16], most of the peaks could be denoted as (00n') which come from not single crystal phase but "thin film phase". Only small peak of (002) is observed from the sample heat treated at 50°C for an hour in air. The "thin film phase" thought to be form due to the interaction between the surface of dielectrics and organic layer. Therefore, one can say that the surface state is one of the most important factors of determining the state of organic thin-film. From the results, we confirmed that the heat treatments after film deposition could not lead further crystallization.

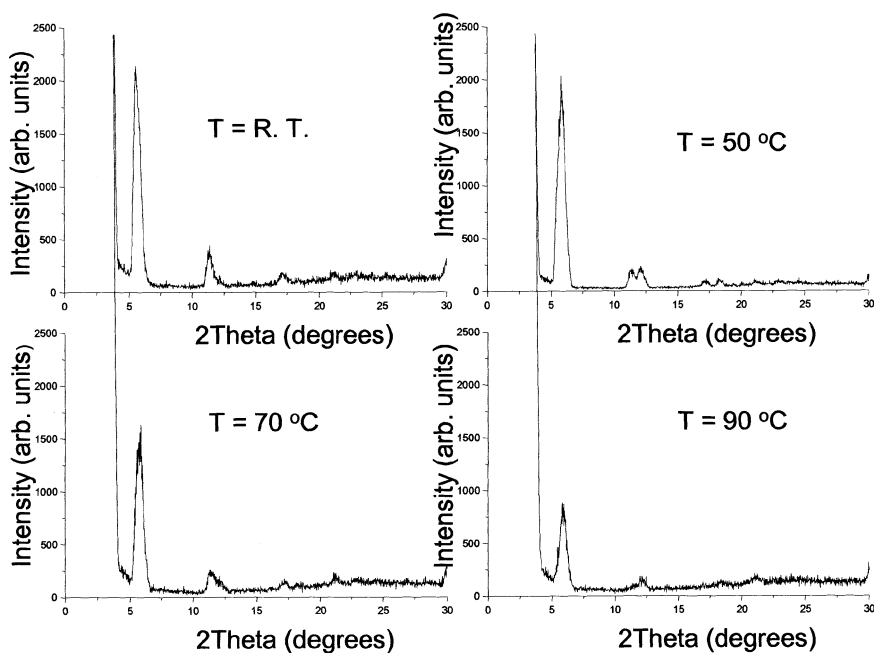


FIGURE 3 XRD patterns of pentacene films deposited on Si/SiO₂ substrates. The samples were heat treated after deposition for further crystallization. Only "thin film phase" is observed.

The characteristic I_{DS} - V_D curves of organic TFT fabricated in this work are shown in Figure 4. The channel width and length are $50\text{ }\mu\text{m}$ and $10\text{ }\mu\text{m}$, respectively, and the thickness of gate dielectrics (SiO_2) is $3000\text{ }\text{\AA}$. When the gate electrode was biased negatively with respect to the grounded source electrode, pentacene TFTs operated in the accumulation mode, and the accumulated charges were holes. The field-effect mobility, which was measured in the saturation regime ($V_D > V_G$) due to the pinch-off of the accumulation layer, was approximately $0.8\text{ cm}^2/\text{Vs}$ calculated with square-law given by

$$I_D = \frac{WC_o}{2L} \mu (V_G - V_T)^2. \quad (1)$$

Linear plot of $I_{DS}^{1/2}$ vs. V_G is shown in Figure 4 as an inset. The on/off ratio of 10^6 were achieved between I_D currents at $V_G = -100\text{ V}$ and $V_G = 20\text{ V}$ measured at a certain V_D in the saturation regime.

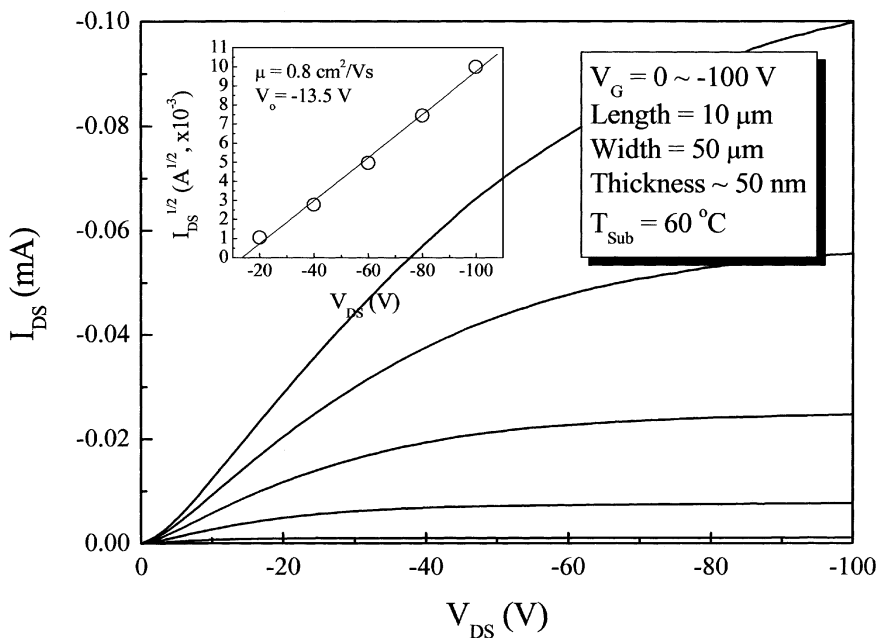


FIGURE 4 I_D - V_{DS} characteristics at various gate voltages for pentacene TFT. On/off ratio is 10^6 .

3.2. Gate Dielectrics

Figure 5(a) shows AFM image of PVA surface fabricated on Au/PET substrate, and AFM image of inorganic layer (Al_2O_3) is also shown in Figure 5(b) for comparison. The measured root-mean-square (RMS) roughness of PVA is 0.76 nm, and it is much smoother than that of the Al_2O_3 layer, 3.23 nm. The transport properties of organic thin film transistors are determined not only by the crystal state of the organic semiconductor thin-film but also by morphology of the gate dielectrics. The effective mobility in polycrystalline materials is given by [17,18]

$$\frac{1}{\mu_{\text{effective}}} = \frac{1}{\mu_L} + \frac{1}{\mu_I} + \frac{1}{\mu_S} + \frac{1}{\mu_D} + \frac{1}{\mu_{\text{GrainBoundary}}} \quad (2)$$

Here, μ_L and μ_I are phonon scattering and impurity scattering, respectively; μ_S is interface roughness scattering, μ_D is defect scattering, and μ_{GB} is grain boundary scattering. As we could obtain smoother surface as well as low leakage current with PVA, we could expect high μ_S .

Figure 6 shows the surface morphologies of gate dielectrics; (a) clean PEN film, (b) Al_2O_3 fabricated on PEN film, (c) JSS-362 on PEN, and (d) Al_2O_3 /JSS-362 on PEN. Figure 6(a) shows the surface of a bare pre-cleaned PEN film and the surface is quite rough like any other commercial plastic film. Figure 3(b) is the image of the Al_2O_3 layer deposited directly on bare PEN film, and Figure 6(d) is the image of the Al_2O_3 layer on

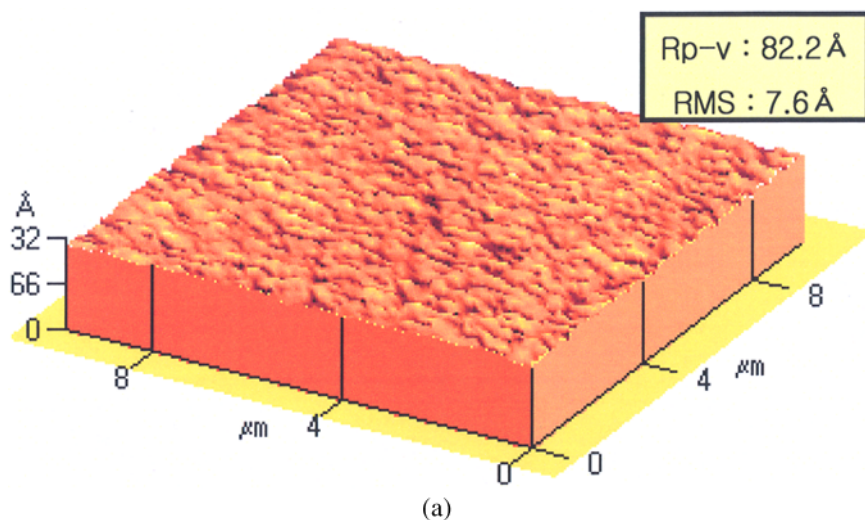


FIGURE 5 AFM image of (a) PVA surface fabricated on Au/PET substrate and (b) inorganic layer (Al_2O_3). The RMS roughness of PVA is 0.76 nm, and it is much smoother than that of the Al_2O_3 layer, 3.23 nm. (See COLOR PLATE V)

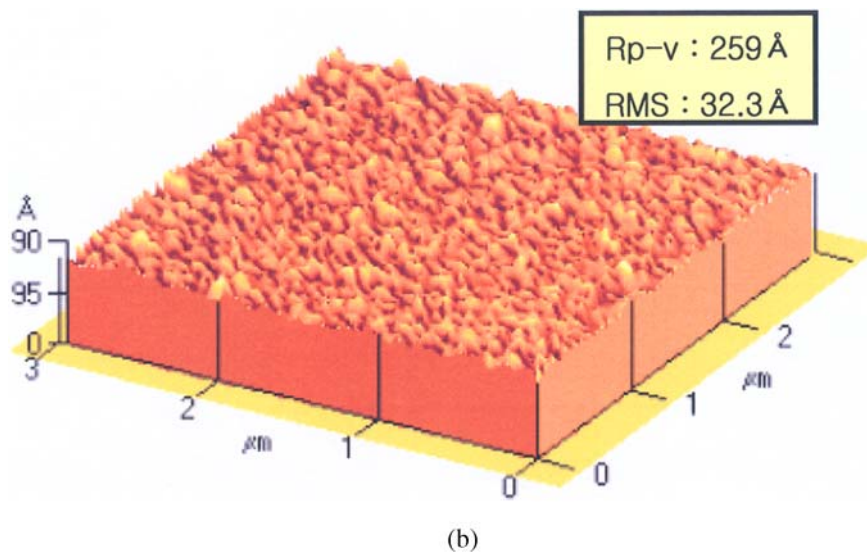


FIGURE 5 (Continued). (See COLOR PLATE VI)

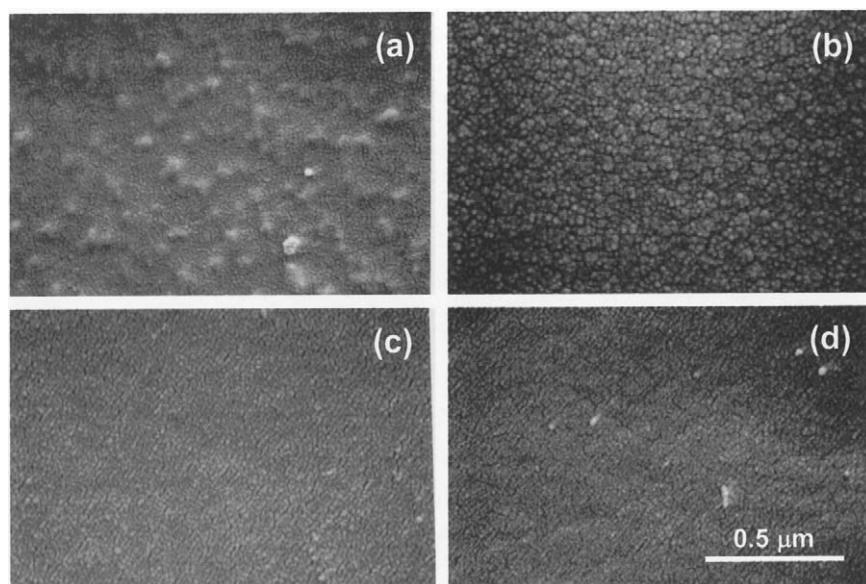


FIGURE 6 The surface morphologies of gate dielectrics; (a) clean PEN film, (b) Al_2O_3 fabricated on PEN film, (c) JSS-362 on PEN, and (d) Al_2O_3 /JSS-362 on PEN observed by scanning electron microscope (SEM).

pre-coated the JSS-362 layer on PEN. Comparing Figure 6(b) and Figure 6 (d), the surface of Al_2O_3 on JSS-362 is much smoother than that of the Al_2O_3 layer on bare PEN. Therefore we can say that the JSS-362 acts as not only dielectric layer but also surface smoothing layer. RMS roughness of the JSS-362 film is quite similar with that of the PVA film, shown in Figure 5 (a).

Figure 7(a) and (b) show the I_D - V_{DS} characteristics of the organic thin-film transistors with gate dielectrics of JSS-362(500 nm)/AlON(100 nm) and PVA(500 nm), respectively. They showed typical transistor characteristics. However, from non-linear behaviors of the drain current at low V_{DS} , one can say that non-ohmic contacts between source-and drain-contact and organic semiconductor were observed. The field effect mobility μ of sample (a) was calculated as $1.4 \times 10^{-2} \text{ cm}^2/\text{Vs}$ by the Eq. (1), while the threshold voltage V_T was about -7 V . The I_{on}/I_{off} ratio was above 10^3 when V_G was scanned from -50 V to $+30 \text{ V}$. For sample (b), μ , V_T , and I_{on}/I_{off} ratio were revealed as $0.12 \text{ cm}^2/\text{Vs}$, -7 V , and 10^4 , respectively.

3.3. Surface Treatments of Source- and Drain-contact with SAMS

Figure 8 shows the chemical structures and the names of the materials used as SAMs on Au, and the work functions of the untreated and the treated Au surfaces by SAMs. Comparing with the work function of bare Au, those of the surface treated by SAMs shifted up to 5.03 eV or down to 4.77 eV resulting in the difference of 0.26 eV . The work functions of these samples were measured by using Riken Keiki Ac-2 in ambient condition.

Figure 9(a) shows the electrical characteristics of the untreated sample with organic semiconductor of pentacene. It shows the typical electric characteristics of a field-effect transistor. The ionization potential of crystalline pentacene film is 4.85 eV [19], and the work function of Au source- and drain-electrode, measured in this work, is also 4.85 eV . Since the energy gap between these two is zero (actually, very small) the drain-source current, I_{DS} , at small drain bias, V_D , is supposed to be small and ohmic [12]. However, as shown in Figure 9(a), non-linear curvature is observed at small V_D . This indicates that the contacts between the source- and drain-electrode and the organic active layer is not ohmic. Watkins *et al.* reported that an interface dipole of -0.97 eV is formed at the pentacene/Au interface with no chemical reactions or interface 'band-bending' [11]. This bad contact is a kind of obstacles for the charge to inject into the organic semiconductor from the metal electrodes. The charge mobility of the device is calculated to be $0.1 \text{ cm}^2/\text{Vs}$ by using Eq. (1). On/off ratio and threshold voltage are about 10^5 and -9 V , respectively.

Figure 9(b) shows the electrical characteristics of the untreated sample with F_{16}CuPc . It also shows the typical electric characteristics of a n-type

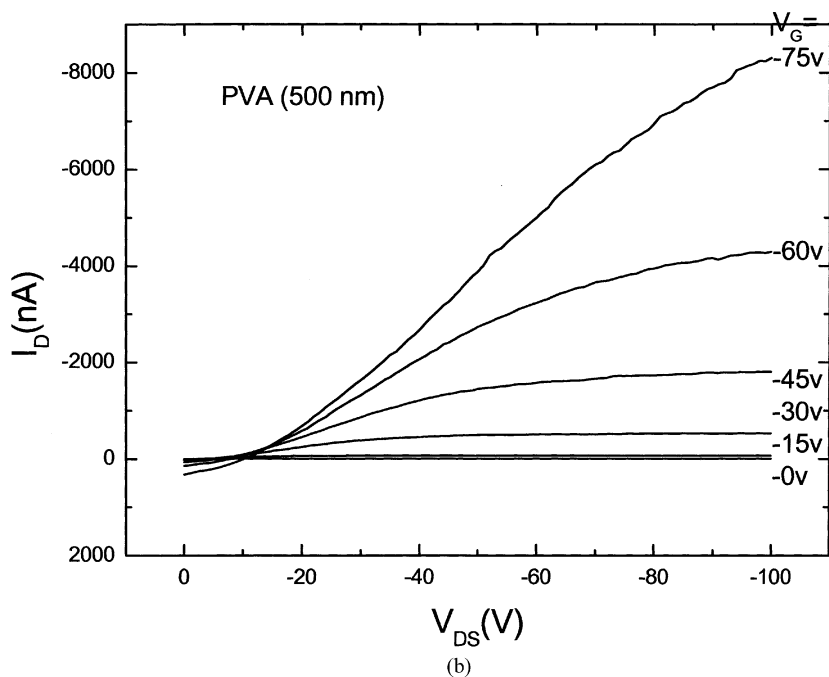
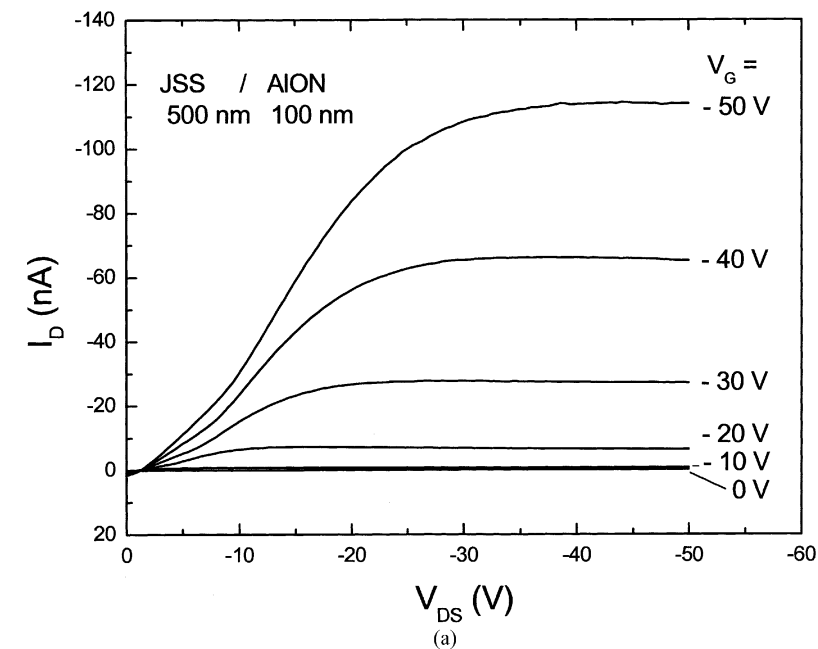


FIGURE 7 The I_D - V_{DS} characteristics of the organic thin-film transistors with gate dielectrics of (a) JSS-362(500 nm)/AlON(100 nm) and (b) PVA(500 nm), respectively.

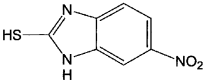
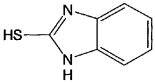
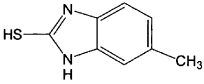
Structure	Name	Work Function (eV)
Au	Gold	4.85, 4.86 (Au)
	6-Nitro-1 <i>H</i> -benzimidazole-2-thiol MNB	5.02, 5.04 (Au/MNB)
	1 <i>H</i> -Benzimidazole-2-thiol MB	4.76, 4.78 (Au/MB)
	6-Methyl-1 <i>H</i> -benzimidazole-2-thiol MMB	4.80, 4.80 (Au/MMB)

FIGURE 8 The chemical structures and the names of the materials used as SAMs on Au, and the work functions of the untreated and the treated Au surfaces by SAMs. The work functions of these samples were measured by using Riken Keiki Ac-2 in ambient condition.

field-effect transistor. The work function difference between Au and general n-type organic semiconductors is about 1 eV [20]. Suprisingly, even though the energy gap between these two is suppose to be about 1 eV, the drain current at small drain bias looks like almost ohmic. The charge mobility of the device is calculated to be $4.3 \times 10^{-4} \text{ cm}^2/\text{Vs}$. On/off ratio, subthreshold slope, and threshold voltage are about 10^4 , 11 V/decade, and 25 V, respectively.

Figure 9 (c) represents the electrical characteristics of the organic field-effect transistors with pentacene and with the Au surface which is treated by SEM using MNB. We can say that much better contact (ohmic contact) was formed between the organic active layer and source- and drain-electrode, because I_D increase almost linearly at low V_{DS} . The saturation current at $V_G = -100 \text{ V}$ is also more than four times larger than that of the untreated sample. The charge mobility at saturation region is calculated as $0.48 \text{ cm}^2/\text{Vs}$. On/off ratio and threshold voltage are over 10^5 and -10 V , respectively.

Figure 9(d) represents the electrical characteristics of the organic field-effect transistors with the Au surface treated by SAM using MNB with organic semiconductor of F_{16}CuPc . The saturation current at $V_G = -100 \text{ V}$ is more than ten times larger than that of the untreated sample. The charge mobility at saturation region is calculated as $4.8 \times 10^{-3} \text{ cm}^2/\text{Vs}$. On/off ratio,

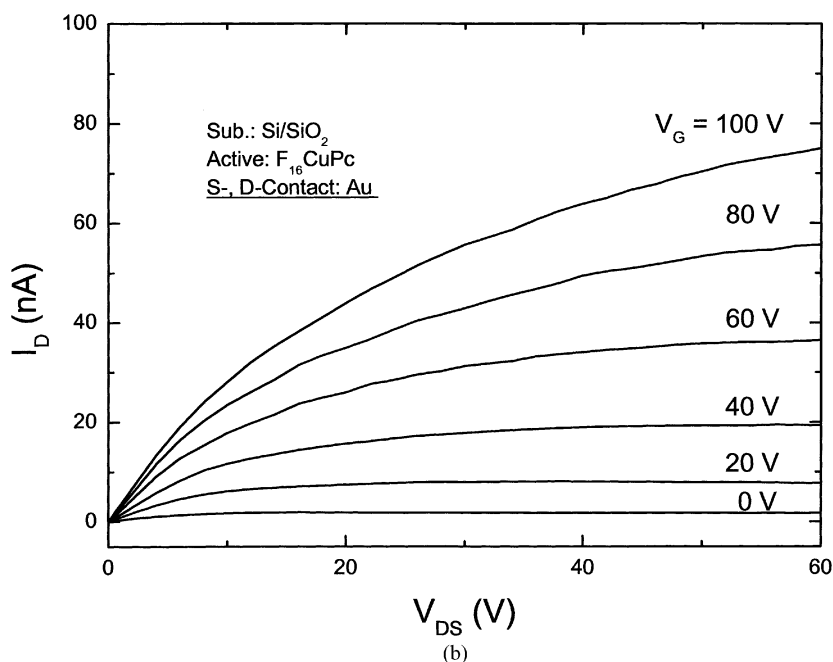
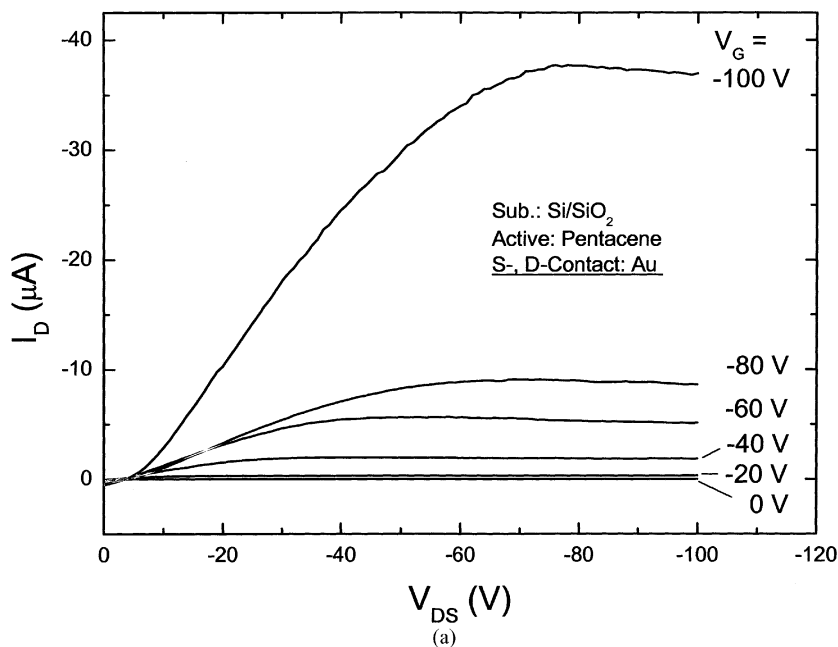


FIGURE 9 The electrical characteristics of the organic TFTs. (a) semiconductor: pentacene, contact treatments: non, (b) semiconductor: F₁₆CuPc, contact treatments: non, (c) semiconductor: pentacene, contact treatments: SAM with MNB, (d) semiconductor: F₁₆CuPc, contact treatments: SAM with MNB.

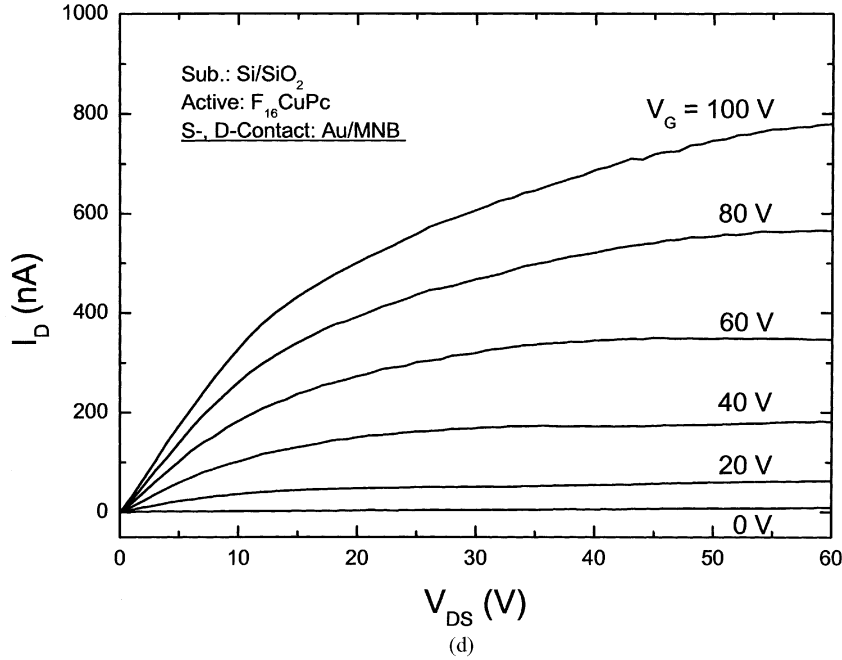
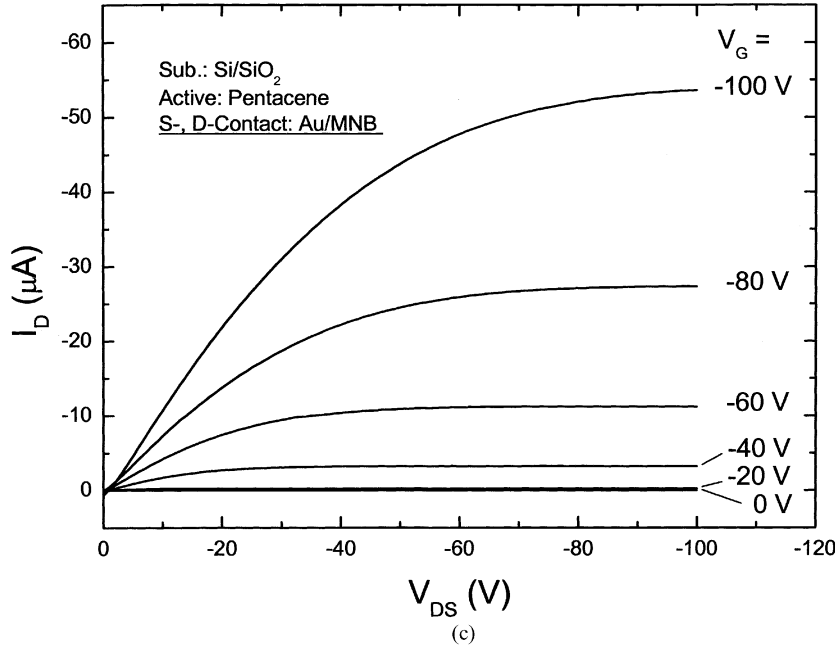


FIGURE 9 (Continued).

TABLE 1 Characteristic Parameters of the Device with p-Type Pentacene

Samples	Work function (eV)	$\mu(\text{cm}^2/\text{Vs})$	$V_T(\text{V})$	S.S.(V/decade)	$R_{\text{on/off}}$
MB/Au	4.77	0.25	-7	2.5	1×10^5
MMB/Au	4.8	0.36	-10	5.7	1×10^5
Au	4.86	0.1	-9	3	1×10^4
MNB/Au	5.03	0.46	-10	2.5	1×10^5

TABLE 2 Characteristic Parameters of the Device with n-Type F_{16}CuPc

Samples	Work function (eV)	$\mu(\text{cm}^2/\text{Vs})$	$V_T(\text{V})$	S.S. (V/decade)	$R_{\text{on/off}}$
MB/Au	4.77	1.4×10^{-3}	25	10	1×10^5
MMB/Au	4.8	3.1×10^{-3}	27	7	2×10^4
Au	4.86	4.3×10^{-4}	25	12	1×10^4
MNB/Au	5.03	4.8×10^{-3}	20	10	4×10^4

subthreshold slope, and threshold voltage are about 4×10^4 , 10 V/decade, and 20 V, respectively. The performances of the Organic TFTs were advanced after SAMs treatments for both p-type pentacene and n-type F_{16}CuPc . Device parameters for both pentacene and F_{16}CuPc are shown in Tables 1 and 2, respectively.

IV. SUMMARY

Organic TFTs with p-type pentacene and n-type F_{16}CuPc were fabricated on both Si and plastic substrates. On Si substrates, maximum p-type mobility of $0.8 \text{ cm}^2/\text{Vs}$ was achieved by surface of gate dielectrics treatment with HMDS and by elevating substrate temperature up to 60°C . For plastic substrates, maximum p-type mobility of $0.12 \text{ cm}^2/\text{Vs}$ was achieved. For this sample, JSS-362 was used as a gate dielectrics.

The electrical properties of the organic field-effect transistors with and without modified source- and drain-electrodes by using self-assembly technique with several thiol compounds were investigated. Charge carrier mobilities of the device with both pentacene and F_{16}CuPc were increased after SAMs treatments on metal contacts. This mobility increase is due to the injection current increase caused by lowering contact resistance.

REFERENCES

- [1] Schön, J. H., Kloc, Ch., & Batlogg, B. (2001). *Synth. Metals*, 122, 195.
- [2] Riess, W., Riel, H., Beierlein, T., Brutting, W., Muller, P., & Seidler, P. F. (2001). *IBM J. Res. & Dev.*, 45, 77.

- [3] Friend, R., Burroughes, J., & Shimoda, T. (1999). *Phys. World (UK)*, **12**, 35.
- [4] Schleupen, K., Alt, P., Andry, P., Asaad, S., Colgan, E., Fryer, P., Galligan, E., Graham, W., Greier, P., Horton, R., Ifill, H., John, R., Kaufman, R., Kinishita, H., Kitahara, H., Kodate, M., Lanzetta, A., Latzko, K., Libertini, S., Libsch, F., Lien, A., Mastro, M., Millman, S., Nunes, R., Nywening, R., Polastre, R., Ritsko, J., Rothwell, M., Takasugi, S., Warren, K., Wilson, J., Wisnieff, R., Wright, S., & Yue, C. (1998). *Proceedings of the 18th international display research conference*, Asia Display '98 187.
- [5] Wisnieff, R. R. (1998). *Nature*, **394**, 225.
- [6] Comiskey, B., Albert, J. D., Yoshizawa, H., & Jakobson, J. (1998). *Nature*, **394**, 253.
- [7] Sheridon, N. K. (1978). *U. S. Patent*, **4**, **126**, 854.
- [8] Crone, B., Dodabalapur, A., Lin, Y.-Y., Filas, R. W., Bao, Z., LaDuca, A., Sarpeshkar, R., Katz, H. E., & Li, W. (2000). *Nature*, **403**, 521.
- [9] Katz, H. E., Lovinger, A. J., Johnson, J., Kloc, C., Siegrist, T., Li, W., Lin, Y.-Y., & Dodabalapur, A. (2000). *Nature*, **404**, 478.
- [10] Bao, Z., Lovinger, A. J., & Brown, J. (1998). *J. Am. Chem. Soc.*, **120**, 207.
- [11] Watkins, N. J., Le, Q. T., Zorba, S., Yan, L., Gao, Y., Nelson, S. F., Cuo, C. S., & Jackson, T. N. (2001). *Proceedings of SPIE*, **4466**, 1.
- [12] Brown, A. R., Jarrett, C. P., de Leuw, D. M., & Matters, M. (1997). *Synthetic Metals*, **88**, 37.
- [13] Wang, J., Gundlach, D. J., Kuo, C. C., & Jackson, T. N. (1999). *41st Electronic Materials Conference Digest*, p16.
- [14] Matters, M., de Leeuw, D. M., Vissenberg, M. J. C. M., & Drury, C. J. (1999). *Opt. Mater.*, **12**, 189.
- [15] Campbell, R. B., Robertson, J., & Trotter, J. (1961). *Acta Cryst.*, **14**, 705.
- [16] Lin, Y.-Y., Gundlach, D. J., Nelson, S. F., & Jacson, T. N. (1997). *IEEE Trans. on Electron Devices*, **44**, 1325.
- [17] Orton, J. W. & Powell, M. J. (1980). *Rep. Prog. Phys.*, **43**, 1263.
- [18] Ahmed, S. S., Kim, D. M., & Shichijo, H. (1985). *IEEE Electron Device Lett.*, **6**, 313.
- [19] Sato, N., Seki, K., Inokuchi, H., & Harada, Y. (1986). *Chem. Phys.*, **109**, 157.
- [20] Dimitrakopoulos, C. D., & Malenfant, P. R. L. (2002). *Adv. Mat.*, **14**, 99.